

# Neural Graph Matching Network: Learning Lawler’s Quadratic Assignment Problem with Extension to Hypergraph and Multiple-graph Matching

Runzhong Wang Junchi Yan\* Xiaokang Yang  
 Shanghai Jiao Tong University  
 Shanghai, China  
 {runzhong.wang, yanjunchi, xkyang}@sjtu.edu.cn

## Abstract

Graph matching involves combinatorial optimization based on edge-to-edge affinity matrix, which can be generally formulated as Lawlers Quadratic Assignment Problem (QAP). This paper presents a QAP network directly learning with the affinity matrix (equivalently the association graph) whereby the matching problem is translated into a vertex classification task. The association graph is learned by an embedding network for vertex classification, followed by Sinkhorn normalization and a cross-entropy loss for end-to-end learning. We further improve the embedding model on association graph by introducing Sinkhorn based constraint, and dummy nodes to deal with outliers. To our best knowledge, this is the first network to directly learn with the general Lawlers QAP. In contrast, state-of-the-art deep matching methods [39, 32, 42] focus on the learning of node and edge features in two graphs respectively. We also show how to extend our network to hypergraph matching, and matching of multiple graphs. Experimental results on both synthetic graphs and real-world images show our method outperforms. For pure QAP tasks on synthetic data and QAPLIB, our method can surpass spectral matching [19] and RRWM [9], especially on challenging problems.

## 1. Introduction and Preliminaries

Graph matching (GM) has been a fundamental problem in computer science which is NP-hard in general [12]. It has various applicability and connection with vision and learning. It involves establishing node correspondences between two graphs based on the node-to-node and edge-to-edge affinity [9, 13]. The problem can be generalized to the higher-order case whereby hyperedges and their affinity [18, 24, 37] are defined for matching. This is in contrast

to the point based methods e.g. RANSAC [11] and iterative closest point (ICP) [41] without explicit edge modeling.

We start with two-graph matching, which can be written as quadratic assignment programming (QAP) [22], where  $\mathbf{X}$  is a (partial) permutation matrix encoding node correspondence, and  $\text{vec}(\mathbf{X})$  is its vectorized version:

$$J(\mathbf{X}) = \text{vec}(\mathbf{X})^\top \mathbf{K} \text{vec}(\mathbf{X}) \quad (1)$$

$$s.t. \quad \mathbf{X} \in \{0, 1\}^{n_1 \times n_2}, \mathbf{X} \mathbf{1}_{n_2} = \mathbf{1}_{n_1}, \mathbf{X}^\top \mathbf{1}_{n_1} \leq \mathbf{1}_{n_2}$$

Here  $\mathbf{K} \in \mathbb{R}^{n_1 n_2 \times n_1 n_2}$  is the so-called affinity matrix [19]. Its diagonal elements and off-diagonal elements store the node-to-node and edge-to-edge affinities. One popular embodiment of  $\mathbf{K}$  in literature is  $K_{ia,jb} = \exp\left(\frac{\|\mathbf{f}_{ij} - \mathbf{f}_{ab}\|^2}{\sigma^2}\right)$  where  $\mathbf{f}_{ij}$  is the feature vector of the edge  $E_{ij}$ .

Note Eq. (1) in literature is called Lawler’s QAP [17], which can incorporate other special forms. For instance, the popular Koopmans-Beckmann’s QAP [22] is written by:

$$J(\mathbf{X}) = \text{tr}(\mathbf{X}^\top \mathbf{F}_1 \mathbf{X} \mathbf{F}_2) + \text{tr}(\mathbf{K}_p^\top \mathbf{X}) \quad (2)$$

where  $\mathbf{F}_1 \in \mathbb{R}^{n_1 \times n_1}$ ,  $\mathbf{F}_2 \in \mathbb{R}^{n_2 \times n_2}$  are weighted adjacency matrices.  $\mathbf{K}_p$  is node-to-node affinity matrix. Its connection to Lawler’s QAP becomes clear by letting  $\mathbf{K} = \mathbf{F}_2 \otimes \mathbf{F}_1$ .

The above models involves second-order affinity. They can also be generalized to the higher-order case. A line of works [7, 10, 37, 40] adopt tensor marginalization based model for  $m$ -order ( $m \geq 3$ ) hypergraph matching:

$$\mathbf{x}^* = \arg \max(\mathbf{H} \otimes_1 \mathbf{x} \otimes_2 \mathbf{x} \dots \otimes_m \mathbf{x}) \quad (3)$$

$$s.t. \quad \mathbf{X} \mathbf{1}_{n_2} = \mathbf{1}_{n_1}, \mathbf{X}^\top \mathbf{1}_{n_1} \leq \mathbf{1}_{n_2}$$

where  $\mathbf{x} = \text{vec}(\mathbf{X}) \in \{0, 1\}^{n_1 n_2 \times 1}$  is the vectorized form, and  $\mathbf{H}$  is the  $m$ -order affinity tensor whose element records the affinity between two hyperedges, operated by tensor product  $\otimes_k$  [18]. Details of tensor multiplication can be referred to Sec. 3.1 in [10]. Most existing hypergraph matching works assume the affinity tensor is invariant w.r.t. the index of the hyperedge pairs for computational tractability.

\*Corresponding author. Runzhong Wang, Junchi Yan and Xiaokang Yang are also with MoE Key Lab of Artificial Intelligence, AI Institute, Shanghai Jiao Tong University.

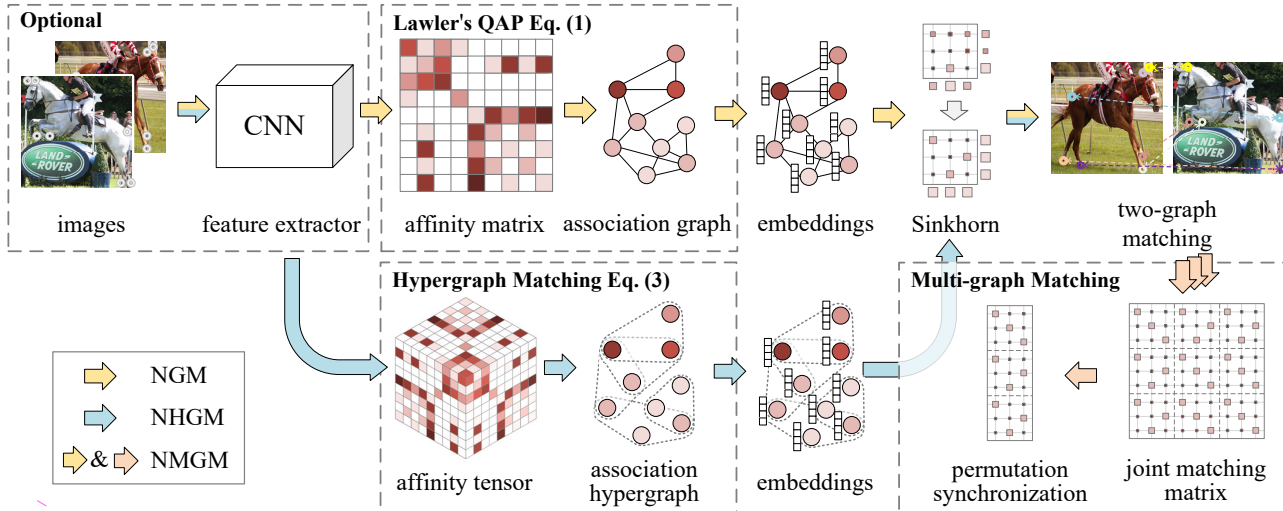


Figure 1. Overview on the proposed neural graph matching pipeline. We further extend it to hypergraph matching to replace the association graph with an association hypergraph, and also to multiple graph matching by permutation synchronization.

Traditional methods mostly assume the affinity is predefined and focus on finding the optimal solution. The limited capacity of a shallow affinity model e.g. Gaussian kernel with Euclid distance, cannot provide enough flexibility for real-world data. In other words, the predefined affinity function can be biased and even the mathematically optimal solution can departure from the perfect matching in reality. Such challenges have also been (partially) addressed in multiple graph matching, which tries to enforce cycle-consistency to conquer local bias [33, 36]. We resort deep network to train the affinity function adapted to data. Our network further learns to solve QAP (and matching of hypergraph as well as multiple graphs) end-to-end.

Our matching nets have several learnable layers: 1) CNN layers taking raw images for node (and edge) feature extraction; 2) affinity metric learning layer for generating the affinity matrix i.e. the association graph; 3) node embedding layers using the association graph as input for vertex classification; 4) Sinkhorn net to convert the vertex score matrix into double-stochastic matrix. In particular, Sinkhorn technique is also adopted in the embedding module to introduce matching constraint; 5) cross-entropy loss layer whose input is the output of the Sinkhorn layer.

Note that the first two components are optional and can be treated as plugin in the pipeline, which have nothing to do with Lawler’s QAP. In contrast, the peer network [39] only allows for learning of node CNN features on images and their similarity metric i.e. the component 1) and 2) in the above setting which is in fact inapplicable to learning the QAP model. Our embedding is also different from [42, 32] as the raw graphs must be taken as input in these works. In fact, [25] shows that embedding on individual graphs can deal with some special cases of Koopmans-Beckmann’s QAP, which is also a special case of Lawler’s QAP.

Our networks are generalized to hypergraph matching by embedding a higher-order affinity tensor, and also to the multiple graph matching case by devising an end-to-end compatible matching synchronization module inspired by [26]. **In a nutshell, the highlights of this paper are:**

i) We show for the first time in literature, how to develop a deep network to directly tackle the (most) general graph matching formulation i.e. Lawlers Quadratic Assignment Problem. This is fulfilled by regarding the affinity matrix as an association graph, whose vertices can be embedded by a deep graph neural network for vertex classification. In contrast, existing works [8, 39, 42, 32] in fact start with the graph’s node and edge features instead of pairwise affinity encoded in the affinity matrix. As shown earlier in this paper, (some of) such models can be bridged to Koopmans-Beckmanns QAP which is a special case of Lawler’s QAP. We also adopt dummy nodes to handle outliers.

ii) We extend our second-order graph matching networks to the hypergraph (third-order) matching case. This is fulfilled by building the hyperedge based association hypergraph to replace the second-order one. To our best knowledge, this is the first work for deep learning of hypergraph matching (with explicit treatment on the hyperedges).

iii) We also extend our matching network to the multiple-graph matching case by end-to-end permutation synchronization. To our best knowledge there is no multiple-graph matching neural network in existing literature.

iv) Experimental results on synthetic and real-world data show the effectiveness of our devised components. The extended versions for hypergraph matching and multiple-graph matching also show competitive performance. Our model can learn with the Lawler’s QAP as input while state-of-the-art graph matching networks [39, 32, 42] cannot.

## 2. Related Work

### 2.1. Learning-free Graph Matching Methods

**Two-graph matching methods.** Graph matching is traditionally addressed in a learning free setting, and mostly for matching of two graphs [9, 3, 43], which can be formulated as QAP. Most methods focus on seeking approximate solution given fixed affinity model which is often set in simple parametric forms. Euclid distance in node/edge feature space, or together with a Gaussian kernel to derive a non-negative similarity, is widely used in the above works.

**Hypergraph matching methods.** Going beyond the traditional second-order graph matching, hypergraphs have been built for matching [40] and their affinity is usually represented by a tensor to encode the third-order [37, 18] or even higher-order information [24]. The advantage is that the model can be more robust against noise at the cost of exponentially increased complexity for both time and space.

**Multiple-graph matching methods.** It has been recently actively studied for its practical utility against local noise and ambiguity. Among the literature, a thread of works [26, 6] first generate the pairwise matching between two graphs via certain two-graph matching solvers, and then impose cycle-consistency on the pairwise matchings to improve the matching accuracy. The other line of methods impose cycle-consistency during the iterative finding of pairwise matchings, and usually can achieve better results [36, 33, 35, 34]. Another relevant setting is solving multiple graph matching in an online fashion [38].

One can observe both hypergraph model or multiple graph matching paradigm try to improve the affinity model either via lifting the affinity order or imposing additional consistency regularization. As shown in the following, another possibly more effective way is adopting learning to find more adaptive affinity model parameters, or further improving the model capacity by adopting neural networks.

### 2.2. Learning-based Graph Matching Methods

**Shallow-learning methods.** The structural SVM based supervised learning method [8] incorporates the earlier graph matching learning methods [30, 5, 20, 30]. In addition, the learning can also be fulfilled by unsupervised [20] and semi-supervised [21]. In these earlier works, no network is adopted until the recent seminal work [39].

**Deep-learning methods.** Deep learning has been recently applied to graph matching [39], whereby convolutional neural network (CNN) is used to extract node features from images followed with spectral matching and the CNN is learned using a regression-like node correspondence supervision. This work is soon improved in [32, 42] by introducing graph neural network to encode the structure information, and devising combinatorial loss based on cross-entropy loss, and Sinkhorn Network [1] as adopted in [32].

One shortcoming of the above graph matching networks is that they cannot directly deal with the most general QAP form which limits their applicability to tasks when individual graph information is not directly available (see <http://coral.ise.lehigh.edu/data-sets/qaplib/>). In contrast, our approach can directly work with the affinity matrix, and we further extend to dealing with affinity tensor for hypergraph matching, as well as the setting under multiple graphs.

## 3. Proposed Approaches

We first present Neural Graph Matching (NGM), which can solve QAP for two-graph matching directly. The enhanced model NGM+ is then devised by adding edge embeddings. We show extension to hypergraph matching, i.e. Neural Hyper-Graph Matching (NHGM), and to multiple graph matching i.e. Neural Multi-Graph Matching (NMGGM). All these three settings to our knowledge have not been addressed by neural network solvers before.

### 3.1. NGM: Neural Graph Matching for QAP

In the following, we denote input graphs by capitals  $G = (V, E)$ , and graph matching can be viewed in a perspective based on the definition of the so-called association graph  $\mathcal{G}^a = (\mathcal{V}^a, \mathcal{E}^a)$  [9, 19] (in handwritten letters). Its vertices  $\mathcal{V}^a = V^1 \times V^2$  represent candidate node-to-node correspondence  $(V_i^1, V_a^2)$ , and edges  $\mathcal{E}^a$  represent the agreement between two pairs of correspondence  $\{(V_i^1, V_a^2), (V_j^1, V_b^2)\}$ , which is often modeled by  $\mathbf{K}_{ia,jb}$ . Its off-diagonal elements  $\mathbf{K}_{ia,jb}$  denote the adjacency matrix of association graph. The matching between two graphs can therefore be transformed into vertex classification on the association graph, following [9, 19]. In this paper, diagonal elements  $\mathbf{K}_{ia,ia}$  are further assigned as vertex attributes  $\mathcal{V}^a$ , to better exploit the first-order similarities. As illustrated in Fig. 2, the association graph prohibits links that violate the one-to-one matching constraint (such as 1a and 1c in Fig. 2(a)).

**Overview.** Neural Graph Matching (NGM) solves QAP in Eq. (1), by vertex classification via graph neural network, specifically Graph Convolutional Networks (GCN) [16] and aggregation based embedding. The vertex classification is performed on the association graph induced by the affinity matrix, followed by a Sinkhorn operator. As shown by existing learning-free graph matching solvers [9, 19], graph matching problem is equivalent to vertex classification on the association graph. NGM accepts either raw image (with CNN), or affinity matrix (without CNN), and learns end-to-end from ground truth correspondence. We follow the protocol in [39, 32] to build the affinity matrix from pre-given keypoints in images, whose image features are extracted by learnable CNN layers. We omit the details of this part to avoid distraction, and readers are referred to [39] for details. In the following, we describe the main steps of NGM.

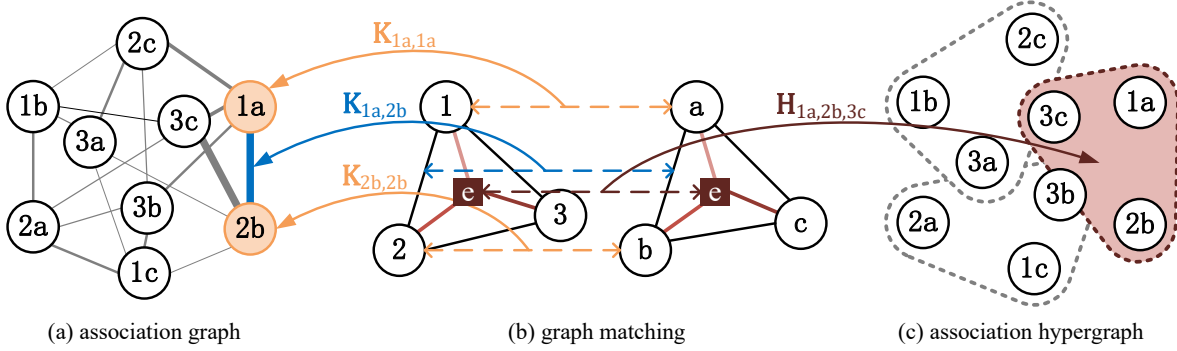


Figure 2. Graphs with affinity matrix  $\mathbf{K}$  and affinity tensor  $\mathbf{H}$ , w.r.t (a) association graph and (c) association hypergraph for embedding. As such the graph matching problem can also be formulated as the vertex classification task on the association graph whose edge weights can be induced by the affinity matrix. Such a protocol is also widely used in literature for graph matching e.g. [9] and hypergraph matching [18].

**Association graph construction.** We derive the association graph that contains vertices and edges, from the affinity matrix in Eq. (1). The connectivity of association graph is represented by off-diagonal elements of affinity matrix  $\mathbf{K}$ . We denote  $\mathbf{v}^{(k)} \in \mathbb{R}^{n_1 n_2 \times l_k}$  as  $l_k$ -dimensional vertex embeddings on GNN layer  $k$ . Initial embeddings are single-dimensional, i.e.  $l_0 = 1$ , taken from diagonal of  $\mathbf{K}$ .

$$\mathbf{W}_{ia,jb} = \mathbf{K}_{ia,jb} \ (ia \neq jb), \quad \mathbf{v}_{ia}^{(0)} = \mathbf{K}_{ia,ia} \quad (4)$$

In case when the first-order similarity  $\mathbf{K}_{ia,ia}$  is absent, we can assign a constant (e.g. 1) for all  $\mathbf{v}^{(0)}$ .

**Matching aware embedding of association graph.** Then the matching problem can be transformed to finding the vertices in the association graph that encode the node-to-node correspondence between two input graphs, as illustrated in Fig. 2. Specifically for vertex classification on the association graph, we use GCN [16] for its effectiveness and simplicity. Firstly, based on (unweighted) adjacency matrix  $\mathbf{A} \in \{0, 1\}^{n_1 n_2 \times n_1 n_2}$ :  $\mathbf{A}_{ia,jb} = 1$  if  $\mathbf{K}_{ia,jb} > 0$  and otherwise 0, we compute the normalized adjacency matrix:

$$\mathbf{A}' = \mathbf{A} \oslash (\mathbf{1}\mathbf{1}^\top \mathbf{A}) \quad (5)$$

The vertex aggregation step is according to:

$$\mathbf{m}^{(k)} = \mathbf{A}' \mathbf{W} f_m(\mathbf{v}^{(k-1)}) + f_v(\mathbf{v}^{(k-1)}), \quad \mathbf{v}^{(k)} = \mathbf{m}^{(k)} \quad (6)$$

where the message passing function  $f_m(\cdot)$  and vertex's self update function  $f_v(\cdot)$  are both implemented by networks with two fully-connected layers and ReLU activation.

The above vanilla vertex embedding procedure in Eq. (6) is general and does not consider the one-to-one assignment constraint for matching. Here we develop a matching constraint aware embedding model: in each layer a soft permutation is predicted via classifier with Sinkhorn network Classifier( $\cdot$ ) (see discussions below) followed by vectorization operator  $\text{vec}(\cdot)$ . The predicted permutation is concatenated to vertex embeddings. Such an embedding scheme is denoted as **Sinkhorn embedding** in the rest of the paper.

$$\mathbf{v}^{(k)} = [\mathbf{m}^{(k)} \quad \text{Classifier}(\mathbf{m}^{(k)})] \quad (7)$$

We experiment both vanilla vertex embedding in Eq. (6) and matching-aware Sinkhorn embedding in Eq. (7), to validate the necessity of adding assignment constraint.

**Vertex classification with Sinkhorn network.** As graph matching is equivalent to vertex classification on association graph (see Fig. 2), a vertex classifier with Sinkhorn network is adopted. We propose a single layer fully-connected classifier denoted by  $f_c(\cdot)$ , followed by exponential activation with regularization factor  $\alpha$ :

$$\mathbf{s}_{ia}^{(k)} = \exp\left(\alpha f_c(\mathbf{v}_{ia}^{(k)})\right) \quad (8)$$

After reshaping classification scores into  $\mathbb{R}^{n_1 \times n_2}$ , one-to-one assignment constraint is enforced to  $\mathbf{s}$  by Sinkhorn network [1, 23], which takes a non-negative square matrix and outputs a doubly-stochastic matrix [1, 27]. As the scoring matrix may be non-square for different sizes of graphs, the input matrix  $\mathbf{S} \in \mathbb{R}^{n_1 \times n_2}$  is padded into a square one (we assume  $n_1 \leq n_2$ ) with small elements e.g.  $\epsilon = 10^{-3}$ . A doubly-stochastic matrix is obtained by repeatedly running:

$$\mathbf{S} = \mathbf{S} \oslash (\mathbf{1}_{n_2} \mathbf{1}_{n_2}^\top \cdot \mathbf{S}), \quad \mathbf{S} = \mathbf{S} \oslash (\mathbf{S} \cdot \mathbf{1}_{n_2} \mathbf{1}_{n_2}^\top) \quad (9)$$

where  $\oslash$  means element-wise division. By taking column-normalization and row-normalization in Eq. (9) alternatively,  $\mathbf{S}$  converges to a doubly-stochastic matrix whose rows and columns all sum to 1. The dummy elements are discarded in the final output, whose column sum may be  $< 1$  given unmatched nodes from the bigger graph. Sinkhorn operator is fully differentiable and can be efficiently implemented by automatic differentiation techniques [28].

**Loss for end-to-end training.** Recall the obtained predicted matrix  $\mathbf{S}$  from the above procedure is a doubly-stochastic matrix. Each of its row can be regarded as a sample for multi-class classification whereby the number of class equals to the number of columns. In this sense, we adopt the cross-entropy used in classification as the final loss, given the ground truth node-to-node correspondence:

$$-\sum_{i=1}^{n_1} \sum_{a=1}^{n_2} \mathbf{X}_{i,a} \log \mathbf{S}_{i,a} + (1 - \mathbf{X}_{i,a}) \log(1 - \mathbf{S}_{i,a}) \quad (10)$$

All the components are differentiable, hence NGM, including optional CNN for keypoint feature extraction from images, is learned via back propagation and gradient descent. We further enable NGM with edge embedding.

### 3.2. NGM+: Improved NGM with Edge Embedding

**Edge embedding.** Edge embedding has been verified effective to enhance vertex embedding learning [14] and we improve NGM with additional edge embeddings, resulting the enhanced method called NGM+.

We extend GCN [16] with  $l_k$ -dimensional edge embedding  $\mathbf{W}^{(k)} \in \mathbb{R}^{n_1 n_2 \times n_1 n_2 \times l_k}$  on layer  $k$ , whose feature is updated from features of the same edge and its adjacent nodes. Initial edge embeddings are single-dimensional, taken from off-diagonal elements of adjacency matrix  $\mathbf{K}$ :

$$\mathbf{W}_{ia,jb}^{(0)} = \mathbf{K}_{ia,jb} \quad (ia \neq jb) \quad (11)$$

Our method starts with edge feature updating from the edge and its adjacent nodes in the previous layer, then concatenated and passed by edge update function  $f_e(\cdot)$ :

$$\mathbf{W}_{ia,jb}^{(k)} = f_e([\mathbf{W}_{ia,jb}^{(k-1)} \quad \mathbf{v}_{jb}^{(k-1)}])_{\forall ia,jb \in \mathbf{K}_{ia,jb} > 0} \quad (12)$$

$f_e(\cdot)$  is a neural network containing two fully-connected layers with ReLU activation. Note that the consistency of edges among all layers is enforced by  $ia, jb \in \mathbf{K}_{ia,jb} > 0$ .

**Embedding of association graph with edges.** Similar to [14], along the third dimension, i.e. feature channels of  $\mathbf{W}^{(k)}$ , edge embeddings are taken for vertex aggregation. The vertex aggregation step is performed as follows:

$$\begin{aligned} \mathbf{m}^{(k)} &= (\mathbf{A}')_3 \mathbf{W}^{(k)} \otimes f_m(\mathbf{v}^{(k-1)}) + f_v(\mathbf{v}^{(k-1)}) \\ \mathbf{v}^{(k)} &= \left[ \mathbf{m}^{(k)} \quad \text{vec}(\text{Classifier}(\mathbf{m}^{(k)})) \right] \end{aligned} \quad (13)$$

where  $(\mathbf{A}')_3$  means expanding along third dimension and  $\otimes$  denotes stacked matrix multiplication along third dimension.  $f_m(\cdot)$  and  $f_v(\cdot)$  are two fully-connected layers with ReLU activation. We also adopt Sinkhorn embedding in NGM+. The other components of NGM+ are consistent with NGM in Sec. 3.1.

### 3.3. NHGM: Neural Hypergraph Matching

For Neural Hyper-Graph Matching (NHGM), the higher order structure is exploited for more robust correspondence prediction. NHGM owns a nearly identical pipeline compared to NGM, while a more general message passing scheme is devised for feature aggregation in hypergraphs. Due to the explosive computational cost ( $O((n_1 n_2)^t)$  with order  $t$ ), here we limit hypergraph to third-order which is also in line with the majority of existing works [37], while the scheme is generalizable to any order  $t$ .

**Association hypergraph construction.** The affinity matrix is generalized to affinity tensor  $\mathbf{H}^{(t)}$  of order  $t$ . In

line with the hypergraph matching literature [40, 18, 10], the third-order affinity tensor is specified as:

$$\mathbf{H}_{\omega_1, \omega_2, \omega_3}^{(3)} = \exp \left( - \left( \sum_{q=1}^3 |\sin \theta_{\omega_q}^1 - \sin \theta_{\omega_q}^2| \right) / \sigma_3^2 \right) \quad (14)$$

where  $\theta_{\omega_q}^1, \theta_{\omega_q}^2$  denotes the angle in graph  $\mathcal{G}_1$  and  $\mathcal{G}_2$  of correspondence  $\omega_q$ , respectively. Readers are referred to Fig. 5 in [18] for an intuitive view of the third-order affinity.

As an extension from the second-order association graph, a hyper association graph is constructed from  $\mathbf{H}$ . The association hypergraph  $\mathcal{H}^a = (\mathcal{V}^a, \mathcal{E}^a)$  takes node-to-node correspondence  $\omega = (V_i^1, V_j^2)$  as vertices  $\mathcal{V}^a$  and higher-order similarity among  $\{(V_{\omega_1}^1, V_{\omega_1}^2), \dots, (V_{\omega_t}^1, V_{\omega_t}^2)\}$  as hyperedges  $\mathcal{E}^a$ , as Fig. 2(c). Elements of  $\mathbf{H}$  are adjacency weights for the association hypergraph accordingly. In NHGM, features are aggregated through hyperedges.

**Matching aware embedding of association hypergraph.** As an extension of Eq. (6), vertex embeddings are updated from all vertices linked by hyperedges in the association hypergraph. Firstly we compute the normalized adjacency tensor of order  $t$ :

$$\mathbf{A}_{\omega_1, \dots, \omega_t}^{(t)'} = \mathbf{A}_{\omega_1, \dots, \omega_t}^{(t)} / (\mathbf{A}^{(t)} \otimes_2 \mathbf{1} \cdots \otimes_t \mathbf{1})_{\omega_1} \quad (15)$$

Then an aggregation scheme extended from Eq. (6) is taken:

$$\begin{aligned} \mathbf{p}^{(k)} &= f_m^{(t)}(\mathbf{v}^{(k-1)}), \quad \mathbf{H}^{(t)'} = (\mathbf{A}^{(t)'} \odot \mathbf{H}^{(t)})_{t+1} \\ \mathbf{m}^{(k)} &= \sum_t \lambda_t \mathbf{H}^{(t)'} \otimes_t \mathbf{p}^{(k)} \cdots \otimes_2 \mathbf{p}^{(k)} + f_v \\ \mathbf{v}^{(k)} &= \left[ \mathbf{m}^{(k)} \quad \text{vec}(\text{Classifier}(\mathbf{m}^{(k)})) \right] \end{aligned} \quad (16)$$

where  $f_v$  abbreviates  $f_v(\mathbf{v}^{(k-1)})$ ,  $\otimes_i$  denotes tensor product by dimension  $i$ ,  $\odot$  denotes element-wise multiply,  $(\cdot)_{t+1}$  means expanding along dimension  $(t+1)$ . Different orders of features are fused by weighted summation by  $\lambda_t$ .

The other modules of NHGM, including classifier and loss function, are identical to NGM. Therefore, NGM can be viewed as a special case of NHGM, where the order is restricted to 2. Note that the edge embedding scheme introduced in Sec. 3.2 is also applicable to NHGM, but we stick to the simple version for cost-effectiveness.

### 3.4. NMGM: Neural Multi-graph Graph Matching

We further explore the potential of learning multi-graph matching. In this paper, we refer to Permutation Synchronization [26] for its effectiveness and simplicity, and most importantly, its capability in end-to-end training. Readers are referred to [26] for its details and theoretical analysis.

**Building joint matching matrix.** Firstly, we obtain initial two-graph matchings by NGM to build a symmetric joint matching matrix  $\mathcal{S}$ . For  $G_i$  and  $G_j$ ,  $\mathcal{S}_{ij}$  is computed

by NGM as the soft (i.e. continuous) matching matrix. For  $m$  graphs,  $\mathcal{S}$  can be built from all combinations of  $\mathbf{S}_{ij}$ :

$$\mathcal{S} = \begin{pmatrix} \mathbf{S}_{00} & \cdots & \mathbf{S}_{0m} \\ \vdots & \ddots & \vdots \\ \mathbf{S}_{m0} & \cdots & \mathbf{S}_{mm} \end{pmatrix} \quad (17)$$

where for the diagonal part of  $\mathcal{S}$ ,  $\mathbf{S}_{ii}$  is identical matrix.

**End-to-end permutation synchronization.** Following [26], multi-graph matching information can be fused by eigenvector decomposition on  $\mathcal{S}$ . As permutation synchronization assumes no outliers, given  $n$  nodes in each graph, we extract the eigenvectors corresponding to top- $n$  eigenvalues of symmetric matrix  $\mathcal{S}$ :

$$\mathbf{U} \mathbf{\Lambda} \mathbf{U}^\top = \mathcal{S} \quad (18)$$

where diagonal matrix  $\mathbf{\Lambda} \in \mathbb{R}^{n \times n}$  contains top- $n$  eigenvalues and  $\mathbf{U} \in \mathbb{R}^{mn \times n}$  are the  $n$  corresponding eigenvectors. The computation of eigenvalues and eigenvectors are differentiable for end-to-end training [31]. Reconstruction of the joint matching matrix can be written as follows:

$$\hat{\mathcal{S}} = m \mathbf{U} \mathbf{U}^\top \quad (19)$$

According to the backward formulation in [31], if there exists non-distinctive eigenvalues, a numerical divided-by-zero error will be caused. This issue usually happens when cycle-consistency is met in the joint matching matrix, and the synchronized matching is nearly identical to the original matching under such circumstances. Therefore, to avoid this issue, we assign  $\hat{\mathbf{S}}_{ij} = \mathbf{S}_{ij}$  if the minimum residual between top- $n$  eigenvalues is smaller than  $\delta$ , e.g.  $10^{-4}$ .

We replace the Hungarian algorithm in [26] by differentiable Sinkhorn network to obtain the final matching result:

$$\bar{\mathbf{S}}_{ij} = \text{Sinkhorn}(\exp(\hat{\alpha} \hat{\mathbf{S}}_{ij})) \quad (20)$$

where  $\hat{\mathbf{S}}_{ij}$  is from  $\hat{\mathcal{S}}$  and  $\exp(\hat{\alpha} \cdot)$  performs regularization for Sinkhorn. Cross-entropy loss in Eq. (10) is applied to each  $\bar{\mathbf{S}}_{i,j}$  for supervised learning.

## 4. Experiments

As our methods can work with either affinity matrix/tensor or raw RGB image as input, we test them on i) synthetic point registration problem, which takes affinity matrix/tensor as input i.e. directly learning with Lawler’s QAP formulation, ii) QAPLIB dataset with large-scale real-world QAP instances where the network learns to minimize the objective score, and iii) matching semantic keypoints in real images, where CNN affinity is jointly learned with QAP solver. In i) and iii), matching accuracy is computed by the percentage of correct matchings among all ground truth matchings. We also perform hypergraph and multiple graph matching tests to evaluate our NHGM and NMGM.

### 4.1. Synthetic Experiment for QAP Learning

In the synthetic experiment, sets of random points in 2D plane are matched by comparison with other state-of-the-art learning-free graph matching solvers. For each trial, we generate 10 sets of ground truth points whose coordinates are in the plane  $U(0, 1) \times U(0, 1)$ . Synthetic points are distorted by random scaling from  $U(s_l, s_h)$  and additive random noise  $N(0, \sigma_n^2)$ . From each ground truth set, 200 graphs are sampled for training and 100 for testing, resulting in totally 2,000 training samples and 1,000 testing samples in one trial. We assume graph structure is unknown to the GM solver, therefore we construct the reference graph by Delaunay triangulation, and the target graph (may contain outliers) is fully connected. Outliers are also randomly sampled from  $U(0, 1) \times U(0, 1)$ . By default there are 10 inliers and no outliers. We construct a same affinity matrix to formulate Lawler’s QAP for all methods.

As existing learning methods [39, 32, 42] cannot handle Lawler’s QAP, we compare learning-free methods: **1) SM.** Spectral Matching [19] considers graph matching as discovering graph cluster by spectral numerical technique; **2) RRWM.** Reweighted Random Walk Matching [9] adopts a random-walk view, and is one of most powerful and popular learning-free matching algorithms. In this experiment, 2nd-order affinity is modeled by  $K_{i_a, j_b} = \exp(-(\mathbf{f}_{ij} - \mathbf{f}_{ab})^2 / \sigma_2^2)$  where  $\mathbf{f}_{ij}$  is edge length  $E_{ij}$ . We empirically set  $\sigma_2 = 5 \times 10^{-7}$  for all experiments. The modeling of 3rd-order affinity follows Eq. (14) with  $\sigma_3 = 0.1$ . We assign hyperparameters  $\alpha = \hat{\alpha} = 20$  and  $\lambda_2 = \lambda_3 = 1$ .

We adopted the Matlab implementation of SM and RRWM provided by [9], while our PyTorch implementation of NGM, NHGM and NMGM includes a 3-layer GNN of 16 channels. NGM-V means vanilla NGM without Sinkhorn embedding (see discussions between Eq. (6) and Eq. (7)) and NMGM-T represents directly transfer pretrained NGM into multi-matching without tuning. Multi-graph matching involves 4 graphs by default. Hungarian algorithm is adopted as the common discretization step.

Fig. 3 shows our proposed NGM surpasses SM and reaches comparative results against the powerful learning-free RRWM. The robustness of hyper matching NHGM becomes significant when we further disturb the matching problem by random scaling (Fig. 3(b)) and outliers (Fig. 3(c)). In Fig. 3(a)(b), NMGM obtains steady improvement by fusing multi-graph information, and in Fig. 3(d) we show the improvement in NMGM by introducing more graphs, and the necessity of learning joint matching as NMGM steadily outperforms NMGM-T whose weights are directly transferred from two-graph NGM. In fact, NGM-V without Sinkhorn embedding works in a way similar to SM as the embedding procedure does not take the assignment constraint into consideration, and they also perform closely to each other. On the other hand, by exploiting Sinkhorn

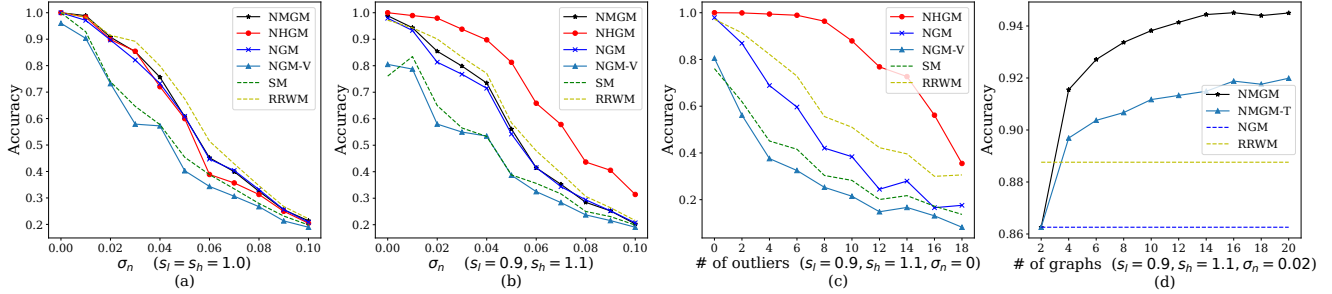
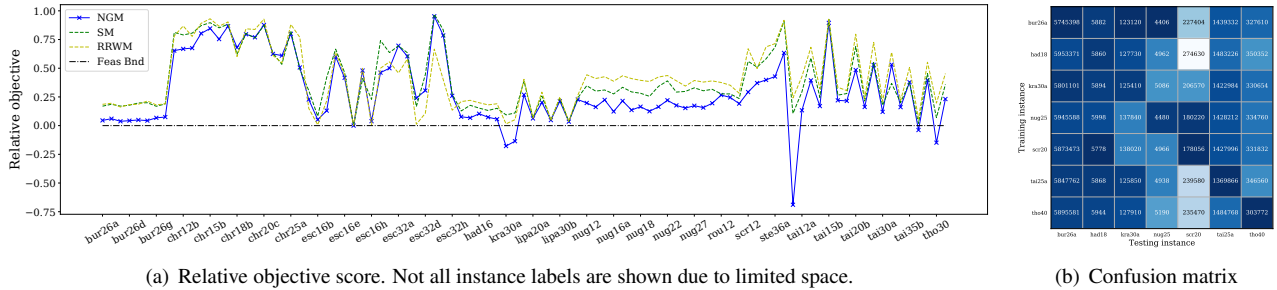


Figure 3. Synthetic test by varying deformation level  $\sigma_n$ , number of outliers and graphs. This test involves purely learning a combinatorial solver for QAP, rather than any affinity model. This feature is not supported in GMN [39] and PCA-GM [32] thus they cannot be compared.



(a) Relative objective score. Not all instance labels are shown due to limited space. (b) Confusion matrix

Figure 4. Relative objective score and generalization test on real-world QAPLIB instances (lower score is better).

embedding, NGM is conceptually similar to RRWM as both methods try to incorporate the assignment constraint on the fly. Interestingly their performances are also very close.

## 4.2. Learning Real-world QAP Instances

Our proposed NGM solves the most general Lawler’s QAP, which has wide range of applications beyond vision. Evaluation on the QAPLIB benchmark [4] is performed to show the capability of NGM on learning the QAP objective score. The QAPLIB contains 134 real-world QAP instances from 15 categories, and the problem size ranges from 12 to 256. However, most of the instances are relatively small, and experiments are conducted on a subset of 95 QAPLIB instances whose sizes are no larger than 40. We modify the loss function into objective score of QAP, keeping the model architecture unchanged. It turns out a self-supervised learning task where the objective score is minimized.

We train one model for each category, and report the relative objective score  $\frac{obj\_score - feas\_bnd}{obj\_score}$  against the up-to-date feasible bound provided by the benchmark<sup>1</sup>. In Fig. 4(a), our method beats RRWM [9] and SM [19] on most problems. As there is no learning based QAP solvers, only non-learning methods are compared. NGM can even surpass the known feasible bound (dashed black line) on certain problems. We also show in Fig. 4(b) that the learned QAP solver generalizes soundly to unseen problems, where models are trained by problems on column and tested on

<sup>1</sup>Feasible bounds are computed from the provided permutation, at <http://coral.ise.lehigh.edu/data-sets/qaplib/qaplib-problem-instances-and-solutions/>

row. The problems are arbitrarily selected. Objective scores are plotted and darker color denotes better performance.

## 4.3. Real Image for Joint CNN and QAP Learning

Our matching net also allows for raw image input, from which a CNN is learned with affinity features. We evaluate semantic keypoint matching on Pascal VOC dataset with Berkeley annotations<sup>2</sup> [2] and Willow ObjectClass [8].

**Pascal VOC Keypoint dataset** contains 20 instance classes with semantic keypoint labels. We follow the problem setting in [32], where image pairs with inlier positions are fed into the model. We consider it a challenging dataset because instance may vary from its scale, pose and illumination, and the number of inliers varies from 6 to 23. The shallow learning method HARG-SSVM [8] incorporates a fix-sized reference graph, therefore is inapplicable to our experiment setting where instances from same category have different inliers. Because Permutation Synchronization [26] requires same number of nodes in multiple graphs, our multi-graph model NMGM is not compared either.

Following the peer methods [39, 32] we filter out poorly annotated images, after which we get 7,020 training samples and 1,682 testing samples. Instances are cropped around their ground truth bounding boxes and resized to  $256 \times 256$  before fed into the network. We adopt VGG16 backbone [29] and construct the affinity matrix from the same CNN layers: relu4.2 for node features and relu5.1 for edge features. Edge features are built by concatenat-

<sup>2</sup>[https://www2.eecs.berkeley.edu/Research/Projects/CS/vision/shape/poselets/voc2011\\_keypoints\\_Feb2012.tgz](https://www2.eecs.berkeley.edu/Research/Projects/CS/vision/shape/poselets/voc2011_keypoints_Feb2012.tgz)

method	aero	bike	bird	boat	bottle	bus	car	cat	chair	cow	table	dog	horse	mbike	person	plant	sheep	sofa	train	tv	mean
RRWM [9]	41.5	54.7	54.3	50.3	67.9	74.3	70.3	60.6	<b>42.3</b>	59.1	48.1	57.3	59.1	56.2	40.6	69.6	63.1	52.2	76.3	87.8	59.3
GMN [39]	31.9	47.2	51.9	40.8	68.7	72.2	53.6	52.8	34.6	48.6	<b>72.3</b>	47.7	54.8	51.0	38.6	75.1	49.5	45.0	83.0	86.3	55.3
PCA-GM [32]	40.9	55.0	<b>65.8</b>	47.9	76.9	<b>77.9</b>	63.5	67.4	33.7	65.5	63.6	61.3	<b>68.9</b>	62.8	44.9	77.5	67.4	57.5	<b>86.7</b>	<b>90.9</b>	63.8
NGM (ours)	50.1	63.5	57.9	53.4	<b>79.8</b>	77.1	73.6	68.2	41.1	<b>66.4</b>	40.8	60.3	61.9	63.5	45.6	77.1	<b>69.3</b>	<b>65.5</b>	79.2	88.2	64.1
NHGM (ours)	<b>52.4</b>	62.2	58.3	55.7	78.7	77.7	<b>74.4</b>	<b>70.7</b>	42.0	64.6	53.8	61.0	61.9	60.8	46.8	<b>79.1</b>	66.8	55.1	80.9	88.7	64.6
NGM+ (ours)	50.8	<b>64.5</b>	59.5	<b>57.6</b>	79.4	76.9	<b>74.4</b>	69.9	41.5	62.3	68.5	<b>62.2</b>	62.4	<b>64.7</b>	<b>47.8</b>	78.7	66.0	63.3	81.4	89.6	<b>66.1</b>

Table 1. Accuracy (%) on Pascal VOC Keypoint. We test our proposed NGM, NHGM, NGM+ with RRWM [9], GMN [39], PCA-GM [32].

method	extra data	face	m-bike	car	duck	w-bottle
HARG-SSVM [8]	×	91.2	44.4	58.4	55.2	66.6
GMN [39]	✓	99.3	71.4	74.3	82.8	76.7
PCA-GM [32]	✓	<b>100.0</b>	76.7	84.0	<b>93.5</b>	96.9
NGM	×	99.2	82.1	84.1	77.4	93.5
NMGM-3-T	×	99.4	84.6	91.3	83.1	94.6
NMGM-6-T	×	99.5	87.3	90.4	82.3	94.3
NMGM-3	×	<b>100.0</b>	84.8	97.2	88.1	94.9
NMGM-6	×	<b>100.0</b>	<b>86.0</b>	<b>97.3</b>	85.4	<b>97.7</b>

Table 2. Accuracy (%) on Willow ObjectClass dataset.

ing feature vectors of starting node and ending node. The affinity score is modeled by weighted inner product of two vectors, containing learnable weights. Readers are referred to [39] for the comprehensive graph construction pipeline. For two input images, one graph is constructed by Delaunay triangulation and the other is fully-connected. Models’ hyperparameters are set identical to previous synthetic tests.

We compare **GMN** [39], **PCA-GM** [32], by which affinity functions are learned for graph matching. Results in Table 1 show that with CNN feature and QAP solver jointly learned, where our methods surpasses competing methods on most categories, especially best performs in terms of mean accuracy. Specifically, NGM surpasses the state-of-the-art deep graph matching method PCA-GM, and it is worth noting that PCA-GM incorporates explicit modeling on higher-order and cross-graph affinities, while only second order affinity is considered in our QAP formulation (and third order for hypergraph matching). NHGM further boost the performance with the help of hypergraph affinities and NGM+ best performs among all methods by exploiting edge embeddings. We also provide result on RRWM, whose affinity matrix is learned by NGM and it solves QAP via RRWM. RRWM outperforms the SM-based learning scheme GMN, but fails to surpass our joint CNN and QAP learning NGM. On single RTX2080Ti, our PyTorch implementation of NGM+ runs at 14.4 samples/sec during training, while NHGM runs at 10.1 samples/sec.

**Willow ObjectClass** contains instances from 5 categories. Each category contains at least 40 images, and all instances in the same class shares 10 distinctive keypoints. We evaluate the effectiveness of joint matching learning of NMGM on Willow ObjectClass dataset. Following the protocol built by [32], we directly train NGM and NMGM on first 20 images and report test result on the rest. The suf-

model	baseline NGM	+ node affinity	+ Sinkhorn embedding
accuracy (rel.)	58.7	59.6 (+0.9)	64.1 (+4.5)
edge embedding	EGNN(C) [14]	HyperConv [15]	Ours Eq. (12)
accuracy	53.3	55.9	<b>66.1</b>

Table 3. Ablation study of NGM+ on Pascal VOC Keypoint.

fix in “NMGM- $k$ ” means learning joint matching among  $k$  graphs, and suffix “T” means transferring NGM weights by adding a permutation synchronization head without learning on joint matching. Performance of HARG-SSVM [8], GMN [39] and PCA-GM [32] reported by [32] are compared, and it’s worth noting that GMN and PCA-GM incorporates additional training data from Pascal VOC Keypoint. Result in Table 2 shows NGM performs comparatively to state-of-the-art PCA-GM, and NMGM surpass PCA-GM by learning multi-graph information. Learning the joint matching on more graphs can achieve further improvement, as NMGM-6 outperforms NMGM-3. But there is little improvement from NMGM-3-T to NMGM-6-T.

#### 4.4. Ablation Study on Pascal VOC Keypoint

Ablation study is performed on proposed modules in NGM+ and experimental result on Pascal VOC Keypoint dataset is shown in Table 3. The baseline model is built following NGM introduced in Sec. 3.1, however node affinity is ignored in model input, i.e.  $\mathbf{v}_{ia}^{(0)} = 1$  and Sinkhorn embedding is excluded. The effectiveness node affinity, Sinkhorn embedding and NGM+’s edge embedding are evaluated by adding them successively to the model. We also test different edge-embedding schemes including EGNN(C) [14] and HyperConv [15], and we find our edge embedding in Eq. (12) achieves the highest accuracy.

## 5. Conclusion

We have presented a graph matching network. There are three highlights to our best knowledge, having not been addressed before: i) The first network for directly learning Lawlers QAP which is graph matching’s most general form with wide range of applications beyond the image based vision tasks. This is in contrast to existing works that works on separate graphs. ii) The first deep network for hypergraph matching which involves third-order edges. iii) The first network for deep learning of multiple graph matching. Extensive experimental results on synthetic and real-world data show the state-of-the-art performance of our approach.



## References

- [1] R. Adams and R. Zemel. Ranking via sinkhorn propagation. *arXiv:1106.1925*, 2011.
- [2] L. Bourdev and J. Malik. Poselets: Body part detectors trained using 3d human pose annotations. In *ICCV*, 2009.
- [3] R. Burkard, M. DellAmico, and S. Martello. *Assignment Problems*. SIAM, 2009.
- [4] R. Burkard, S. Karisch, and F. Rendl. Qaplib—a quadratic assignment problem library. *Journal of Global optimization*, 10(4):391–403, 1997.
- [5] T. Caetano, J. McAuley, L. Cheng, Q. Le, and A. J. Smola. Learning graph matching. *TPAMI*, 31(6):1048–1058, 2009.
- [6] Y. Chen, L. Guibas, and Q. Huang. Near-optimal joint object matching via convex relaxation. In *ICML*, 2014.
- [7] M. Chertok and Y. Keller. Efficient high order matching. *TPAMI*, 2010.
- [8] M. Cho, K. Alahari, and J. Ponce. Learning graphs to match. In *ICCV*, 2013.
- [9] M. Cho, J. Lee, and K. M. Lee. Reweighted random walks for graph matching. In *ECCV*, 2010.
- [10] O. Duchenne, F. Bach, I. Kweon, and J. Ponce. A tensor-based algorithm for high-order graph matching. *TPAMI*, 2011.
- [11] M. A. Fischler and R. C. Bolles. Random sample consensus: A paradigm for model fitting with applications to image analysis and automated cartography. *Commun. ACM*, 1981.
- [12] M. R. Garey and D. S. Johnson. *Computers and Intractability; A Guide to the Theory of NP-Completeness*. 1990.
- [13] S. Gold and A. Rangarajan. A graduated assignment algorithm for graph matching. *TPAMI*, 1996.
- [14] L. Gong and Q. Cheng. Exploiting edge features for graph neural networks. In *CVPR*, 2019.
- [15] J. Jiang, Y. Wei, Y. Feng, J. Cao, and Y. Gao. Dynamic hypergraph neural networks. In *IJCAI*, pages 2635–2641, 2019.
- [16] T. Kipf and M. Welling. Semi-supervised classification with graph convolutional networks. *ICLR*, 2017.
- [17] E. L. Lawler. The quadratic assignment problem. *Management Science*, 1963.
- [18] J. Lee, M. Cho, and K. M. Lee. Hyper-graph matching via reweighted randomwalks. In *CVPR*, 2011.
- [19] M. Leordeanu and M. Hebert. A spectral technique for correspondence problems using pairwise constraints. In *ICCV*, 2005.
- [20] M. Leordeanu, R. Sukthankar, and M. Hebert. Unsupervised learning for graph matching. *IJCV*, 2012.
- [21] M. Leordeanu, A. Zanfir, and C. Sminchisescu. Semi-supervised learning and optimization for hypergraph matching. In *ICCV*, 2011.
- [22] E. M. Loiola, N. M. de Abreu, P. O. Boaventura-Netto, P. Hahn, and T. Querido. A survey for the quadratic assignment problem. *EJOR*, 2007.
- [23] G. Mena, D. Belanger, S. Linderman, and J. Snoek. Learning latent permutations with gumbel-sinkhorn networks. *ICLR*, 2018.
- [24] Q. Ngoc, A. Gautier, and M. Hein. A flexible tensor block coordinate ascent scheme for hypergraph matching. In *CVPR*, 2015.
- [25] A. Nowak, S. Villar, A. Bandeira, and J. Bruna. Revised note on learning quadratic assignment with graph neural networks. In *DSW*, 2018.
- [26] D. Pachauri, R. Kondor, and S. Vikas. Solving the multi-way matching problem by permutation synchronization. In *NIPS*, 2013.
- [27] R. Santa Cruz, B. Fernando, A. Cherian, and S. Gould. Visual permutation learning. *TPAMI*, 2018.
- [28] F. Serratos, A. Solé-Ribalta, and X. Cortés. Automatic learning of edit costs based on interactive and adaptive graph recognition. In *Gbr*. 2011.
- [29] K. Simonyan and A. Zisserman. Very deep convolutional networks for large-scale image recognition. In *ICLR*, 2014.
- [30] L. Torresani, V. Kolmogorov, and C. Rother. Feature correspondence via graph matching: Models and global optimization. In *ECCV*, 2008.
- [31] S. Walter and L. Lehmann. Algorithmic differentiation of linear algebra functions with application in optimum experimental design (extended version). *arXiv preprint arXiv:1001.1654*, 2010.
- [32] R. Wang, J. Yan, and X. Yang. Learning combinatorial embedding networks for deep graph matching. In *ICCV*, 2019.
- [33] J. Yan, M. Cho, H. Zha, X. Yang, and S. Chu. Multi-graph matching via affinity optimization with graduated consistency regularization. *TPAMI*, 2016.
- [34] J. Yan, Y. Li, W. Liu, H. Zha, X. Yang, and S. Chu. Graduated consistency-regularized optimization for multi-graph matching. In *ECCV*, 2014.
- [35] J. Yan, Y. Tian, H. Zha, X. Yang, Y. Zhang, and S. Chu. Joint optimization for consistent multiple graph matching. In *ICCV*, 2013.
- [36] J. Yan, J. Wang, H. Zha, X. Yang, and S. Chu. Consistency-driven alternating optimization for multigraph matching: A unified approach. *IEEE Transactions on Image Processing*, 24(3):994–1009, 2015.
- [37] J. Yan, C. Zhang, H. Zha, W. Liu, X. Yang, and S. Chu. Discrete hyper-graph matching. In *CVPR*, 2015.
- [38] T. Yu, J. Yan, W. Liu, and B. Li. Incremental multi-graph matching via diversity and randomness based graph clustering. In *ECCV*, 2018.
- [39] A. Zanfir and C. Sminchisescu. Deep learning of graph matching. In *CVPR*, 2018.
- [40] R. Zass and A. Shashua. Probabilistic graph and hypergraph matching. In *CVPR*, 2008.
- [41] Z. Zhang. Iterative point matching for registration of free-form curves and surfaces. *IJCV*, 1994.
- [42] Z. Zhang and W. Lee. Deep graphical feature learning for the feature matching problem. In *ICCV*, 2019.
- [43] F. Zhou and F. D. Torre. Factorized graph matching. In *CVPR*, 2012.